Appropriate Photonic Crystal Topology for Appropriate Applications

1st Tamer S. Mostafa
Department of Telecommunication, Faculty of Engineering, Egyptian Russian University,
Cairo, Egypt,
P.O. 11829,
(algwaal@yahoo.com).
Orcid: **0000-0001-6100-7466**

2nd Shaimaa A. Kroush
Department of Telecommunication, Faculty of Engineering, Egyptian Russian University,
Cairo, Egypt,
P.O. 11829,
(shimaa.krosh@gmail.com).

3rd El- Sayed M. El- Rabaie
Department of Electronics and Electrical Communications Engineering, Faculty of Electronic Engineering, Menoufia University,
Menouf, Egypt,
P.O. 32952,
(elsayedelrabaie@gmail.com).

***Abstract*— In this paper, different topologies were discussed and their effect on the design of photonic crystal applications was evaluated. They can be classified into four categories (i.e., ring resonator, self-collimation, waveguide, and cavity-based structures). The figure of merits of each topology and its impact on design modules were explained and compared for two different applications (i.e., half-adder and decoder). Finite difference time domain (FDTD) and plane wave expansion methods are the two numerical approaches that were used to analyze the proposed designs. The truth table for each application was introduced. Comparison tables were organized to discriminate the valued characteristics for each structure. Based on the extracted tables, the appropriate topology can be chosen for the required design application according to the needed characteristic.**

***Keywords*—photonic crystal, half-adder, decoder, ring resonator, self-collimation, waveguide, cavity.**

I. Introduction

The electronic devices were designed from semiconductor materials that represents crystal lattice with periodic potential for electrons propagation [1- 5]. Nowadays, the mandatory needs for high data rate and transferring what is called big data [6, 7]; the electronic devices faced a problem to do that. This challenge let the researchers to look for other technologies to realize the high-speed applications. Different technologies were proposed to achieve this goal such as semiconductor optical amplifiers (SOA) [7, 8], periodically poled lithium niobate (PPLN) waveguides [9-11], and ring resonators [12, 13], electrical to optical conversion (E/O) [14], and photonic crystal [15] are some representation forms.

The advantage of light speed contributes photonic crystal (Ph. Cs.) to provide high speed applications like sensors [16- 19], filters [20, 21], logic gates (i.e., AND, OR XOR [22- 26], multiplexers and demultiplexers [27- 31], flip-flops [32- 35], encoders [36- 38], decoders [39] and half adders [40]. (Ph. Cs.) can be defined as artificial crystals that have highly ordered dielectric materials with adaption of light propagation [15]. It can appear in one-dimensional (1D) [41- 43], two-dimensional (2D) [44- 46], and three-dimensional (3D) [47- 49].

As well as the electronic band gap forbids electrons in a certain region; there was what is called photonic band gap (PBG) that prevents light to present in a particular wavelength range [15]. From the best of our knowledge, it was found that different applications can be designed when changing the basic structure's topology. These topologies can be classified into ring resonator, self-collimation, waveguide, and cavity. All of them could be shown in square [50] or hexagonal [51] lattice type. For the ring resonator topology, one or more rings can be provided with different size and materials to obtain the resonance wavelength [52]. Line defect was used in self-collimation by changing the radius of rods or holes that built the given module [53]. In the other way, the term point defect was used to form cavity-based structures at the prescribed wavelength [54]. The removal of some rods from the structure will yield a waveguide that will help for passing light to reach the output port [55, 56].

In this paper, two (Ph. Cs.) applications (i.e., half-adder and decoder) were carefully studied to discriminate between the stated topologies' performance such as contrast ratio (C.R.), bit rate, linearity, size, and design simplicity. Different software packages were used to simulate and analyze (Ph. Cs.) structures such as RSOFT [57], COMSOL [58].

This paper is organized as follows. Section 2 covers the detailed study about the photonic crystal topologies and their evaluation metrics. Section 3 and 4 review the main topologies for decoder and half-adder applications. Section 5 presents the extracted comparative study. The conclusions are presented in section 6 followed by the more relevant references.

II. Photonic Crystal Topologies

The (Ph. Cs.) topologies can be classified into four categories ring resonator, self-collimation, waveguide, and cavity. The main parameters that will affect their shape and operation are lattice constant (a) (i.e., the distance between the center of two rods) [15], rode radius (r), and the refractive index (n). Square and hexagonal lattice types were used to implement these structures. This paper was concerned with the comparison between these topologies in two (Ph. Cs.) applications (i.e., half- adder and decoder).

Each topology affects the amount of data transmission per second, which is the bit rate. Response time can be defined as the time required for the output to gain the 90% of its steady-state value from the initiation of the input that caused the change in the output.

The second parameter is the contract ratio (CR) which is defined as the ratio between the power at the lowest logic-1

to that of the highest logic-0 [59]. It is normally expressed as in:

$$CR = 10log\ (p_1/p_0)\ (dB) \quad (1)$$

where P_1 and P_0 refer to the signal power levels at the output port for logic-1 and logic-0, respectively. In the following sections an organized review will be represented for (Ph. Cs.) decoder and half adder from the point of view structure topology.

III. Photonic Crystal Decoder Topologies

Decoder is considered one of the important combinational circuits. The number of input ports is y, and the number of output ports is 2^y at which one and only one will be active [60]. This let the circuit to operate in the applications that needs selectivity such as devices that connected on the computer address bus [61]. The familiar (Ph. Cs.) decoders were seen in 1x2 [62, 63], 2x4 [39, 64], and 3x8 [65] dimension. The truth table for the 2x4 decoder can be shown in table. I.

Table I. Truth tables of the proposed decoder.

Input		Output			
A	B	Q1	Q2	Q3	Q4
0	0	0	0	0	1
0	1	0	0	1	0
1	0	0	1	0	0
1	1	1	0	0	0

As seen in literature, all the proposed decoders operate in the C-band that exists between 1530 to 1565 nm wavelength range [15, 61]. Silicon (Si), chalcogenide glass, and air are the usable materials that were used to build these structures with 3.46, 3.1, 1 refractive indices, respectively. Different lattice types were shown (i.e., square [66], hexagonal [67]). Most of this application were designed to behave in nonlinear regime [39, 68], but some of them were achieved in linear [66, 69]. The auxiliary input was a mandatory need to the majority of these designs [60, 70].

The target of this paper is to study the effect of the topology types on the response of the proposed applications. So it will be discussed in the following sections.

The ring resonator (R. R.) topology was used in (Ph. Cs.) decoders as shown [71- 75]. It constructed by removing rods that arranged in square or hexagonal shape as shown in fig. 1.

The operation is based on adjusting the resonance frequency by changing the position [68, 70], material [72, 73], and the size of ring resonator rods [63]. Moreover, the number of rings affects the output and performance [39, 68, 71].

It can be more classified into hexagonal and square lattice structures [70, 74] as in fig. 1. By combining nonlinear rods in the ring resonator, it can be altered the route of the light [72]. The area for these structures (i.e., with (R.R.)) can be varied between 380.24 μm^2 [70] and 1520 μm^2 [64], so they have large size, and considered as the complex designs.

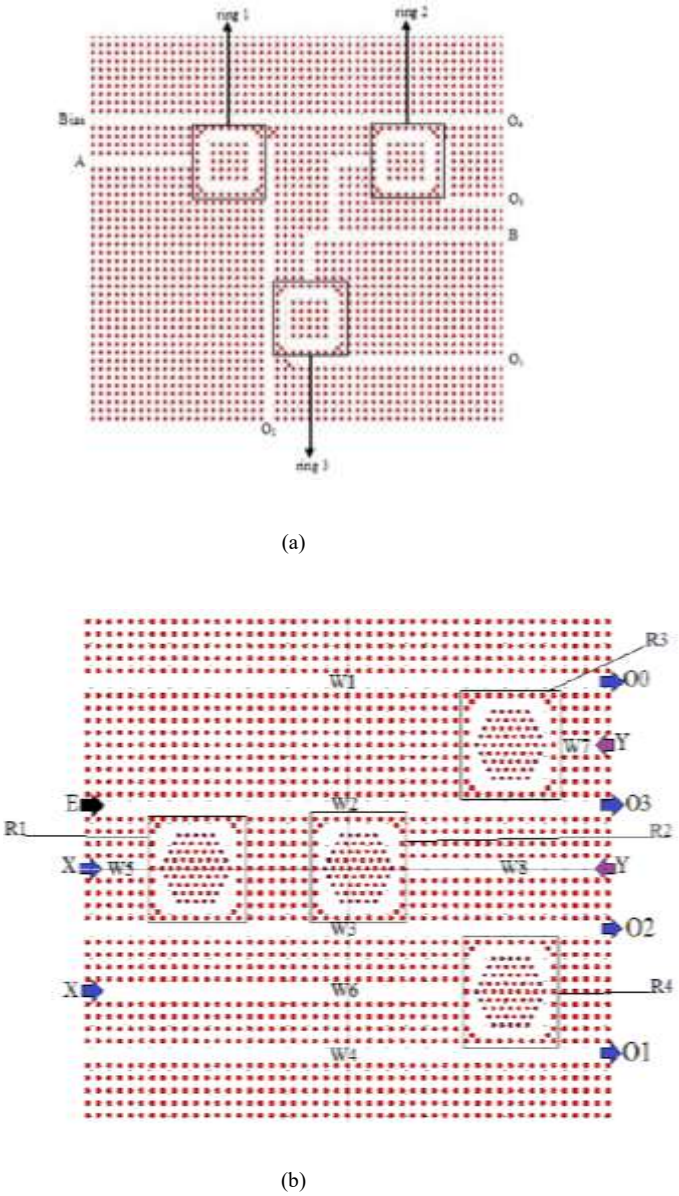

(a)

(b)

Fig. 1. The schematic diagram of the ring resonator of decoder (a) square-ring [70]. (b) hexagonal ring [74].

The second topology that can be found in literature is the self-collimation topology. The operation depends on the incident of light in a plan wave that can propagate along specific direction through a structure by using total internal reflection (TIR) phenomena. The (TIR) happens when the angle of incidence is greater than the critical angle [76].

The self-collimation happens when changing material or radius and lattice constant [69] for one or more rods as in fig. 2. The desired output can be oriented by the angle and the incident light position.

Different materials can be used to introduce splitting plans as shown in fig. 2 to direct the wave in a certain path [50, 69]. From the best of our knowledge, this topology works in the linear regime. The disadvantage of (S.C) that (CR) is poor, where it was around 3.01dB [69].

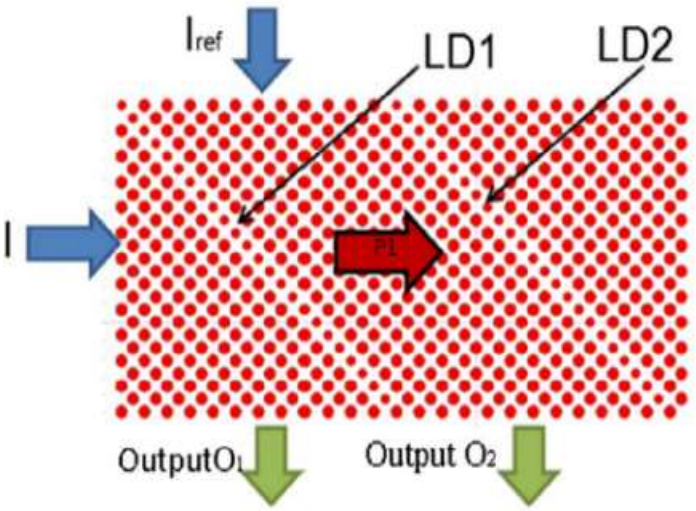

Fig. 2.The schematic diagram of the self-collimation of decoder [69].

Minimum size and simple structures could be represented by this topology.

Waveguide topology is the third one that will be introduced. It can be used to build some structures such as decoders [67, 75]. The waveguide was considered the common section in some topologies [54, 62, 75] because it represents the path for input and output signal as shown in fig. 3. Width, length, and rod's radius are the main parameters that should take into consideration when building structures with this topology [77, 78]. It can be existed in the following shapes cross over [79, 80], T- shape [81], Y-shape waveguides [67, 75, 82, 83].

The arrangement of waveguide arms controls the lunching power to represent the required application [75]. Scattering rods can exist in specific locations to adjust the operating wavelength [84]. Simple designs with high (CR) and bit rate can be obtained from this topology.

As shown in [75], the waveguide decoder with square lattice has an area of 90 μm^2, (CR) equal 13.37dB, and a bit rate of 1587.3 Gbps. On the other hand, the hexagonal type of this topology [67] has a footprint, (CR), bit rate of 234 μm^2, 11.3 dB, and 625 Gbps, respectively.

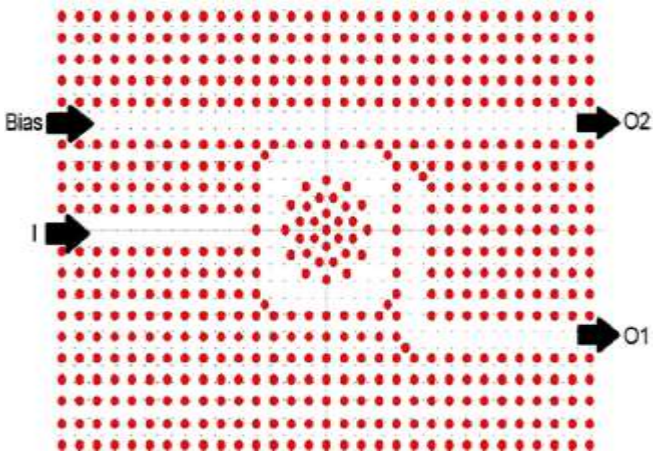

Fig. 3. The schematic diagram of the waveguide of decoder [63].

The last topology that exists in this review was the cavity topology. It is utilized what is called point defect which occurs by removing one rod or hole to obtain the necessary operating wavelength. Moreover, the place of the cavity and its size will affect the resonance [54]. It can play the role of absorbing wave in the forbidden direction [66] and changing the intensity of the incident light. It can be combined with waveguide and ring resonator. The structure that using cavity topology is very simple and has very high (CR) that reach to 16.43dB [66].

Table. II. was organized to display the main difference between the characteristics of (Ph. Cs.) decoders for the proposed topologies.

IV. Photonic Crystal Half-Adder Topologies

One of the important basic circuits that are used in the arithmetic logic unit (ALU) is the half-adder. It combines two inputs to provide two outputs. One is called sum and the other is named carry. The operation was based on the following Boolean equation as in [40]:

$$S=A \oplus B \quad (2)$$

$$C = A \times B \quad (3)$$

These equations will lead to the states in Table. III.

TABLE. III. TRUTH TABLES OF THE PROPOSED HALF-ADDER.

Input		Output	
A	**B**	**Sum(S)**	**Carry(C)**
0	0	0	0
0	1	1	0
1	0	1	0
1	1	0	1

TABLE.II. COMPARISONS BETWEEN THE PUBLISHED ALL-OPTICAL DECODER TOPOLOGIES IN THE LITERATURE

Reference Number	Topology	Dimension	Type	Simplistically	Phase Shifter	Auxiliary Inputs	Lattice Type	Size(μm2)	Bit Rate (GBPs)	Contrast Ratio (dB)	Spectral Wavelength Width (nm)
Ref [39] (2016)	ring resonator	2*4	Nonlinear	X	X	√	Square	1513.7	NA	NA	1483 <λ<1946
Ref [60] (2017)	ring resonator	1*2	Nonlinear	√	X	√	Square	595.35	833.3	7.2	1500 <λ < 2100
Ref [63] (2014)	ring resonator	1*2	Nonlinear	√	X	√	Square	258.35	NA	5.9	1500< λ < 2100
Ref [64] (2017)	ring resonator	2*4	Nonlinear	X	X	√	Square	398.7	NA	6.3	671 < λ < 678
Ref [65] (2020)	ring resonator	3*8	Nonlinear	X	X	√	Square	1742.24	256.4	2.1	NA
Ref [68] (2017)	ring resonator	2*4	Nonlinear	X	X	√	Square	512	166.6	5.68	1324.5 <λ < 1634.8
Ref [70] (2018)	ring resonator	2*4	Nonlinear	X	X	√	Square	380.24	500	5.44	1345.3 < λ <1869.1
Ref [71] (2014)	ring resonator	2*4	Nonlinear	X	X	√	Square	434.24	NA	8	1455 < λ < 1656.
Ref [72] (2020)	ring resonator	2*4	Nonlinear	X	X	√	Square	850	400	10.6	1400 < λ <2100
Ref [73] (2018)	ring resonator	2*4	Nonlinear	√	X	√	Square	368	500	28.7	1480≤ λ ≤2180
Ref [74] (2017)	ring resonator	2*4	Nonlinear	√	X	√	Square	581	NA	NA	1245 n < λ <1875
Ref [69] (2016)	Self-collimation	1*2	linear	√	√	√	square	700	NA	3.01	NA
Ref [67] (2019)	waveguides	1*2	linear	√	√	√	hexagonal	234	625	11.3	1470 < λ <1720
Ref [75] (2019)	waveguides	2*4	Nonlinear	√	X	X	square	90	1587.3	13.37	1215<λ<1710
Ref [54] (2020)	waveguide/cavity	2*4	Nonlinear	√	X	√	square	76	3.33	13.52	1216 < λ < 1701
Ref [66] (2015)	ring/cavity	2*4	linear	X	X	√	square	1520	62.5	16.43	1465 < λ <2032

In this study, it will regard to all (Ph. Cs.) half-adders. As shown in their structures it could be found in square [51, 84, 85] and hexagonal [40, 86, 87] lattice type. Most of them operate in C-band except some of the oldest design that behaved in the lower bands [88]. All the available structures were built in a background of air except that proposed in [87] that has SiO_2 with refractive index of 1.45. Lithium Niobate (LiNbO3, LN) [89], Indium Phosphide, Chalcogenide glasses [86], GNS, and SiO_2 [90] are different materials that used to implement rods. Metal- dielectric was used to verify the operation as in [91]. Auxiliary input was needed in some modules to verify half-adder as in [88, 92].

As shown in fig. 4, the most complex and largest size belonged to the ring resonator topology with 1056 μm^2 as in [51]. On the other hand, the poorest (CR) (i.e., 4.7dB [93]) and simplest structure could be implemented by self-collimation topology as shown in fig. 5. The highest (CR) can be obtained from cavity (i.e., 23 dB [89]) and waveguide topologies (i.e., 16dB [94]) as in fig. 6. Furthermore, remarkable bit rate could be found from the same topologies (i.e., 1.27 Tbsp for cavity [81]) as shown in fig. 6, and 4.550 Tbsp for waveguide [83].

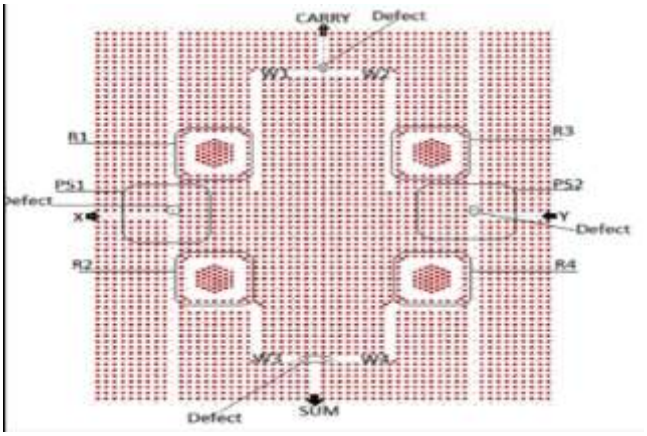

(a)

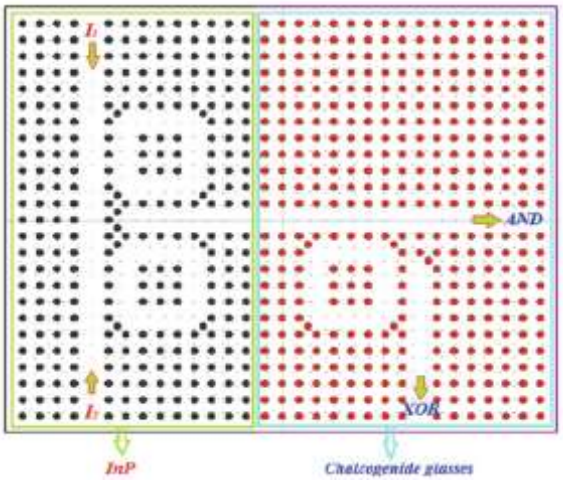

(b)

Fig. 4. The schematic diagram of the ring resonator of half-adder (a) hexagonal ring [51]. (b) square ring [86].

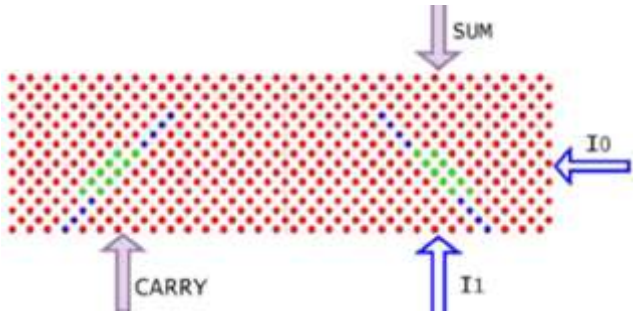

Fig. 5. The schematic diagram of the self-collimation of half-adder [50].

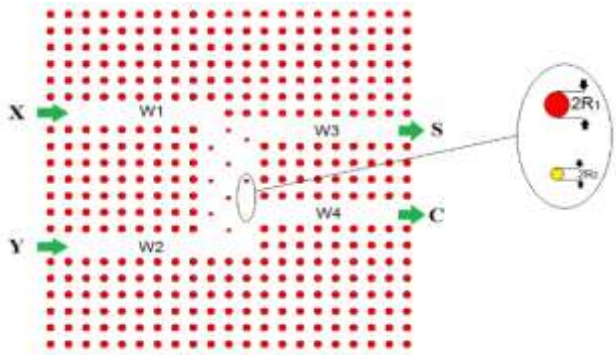

Fig. 6. The schematic diagram of the waveguide of half-adder [94].

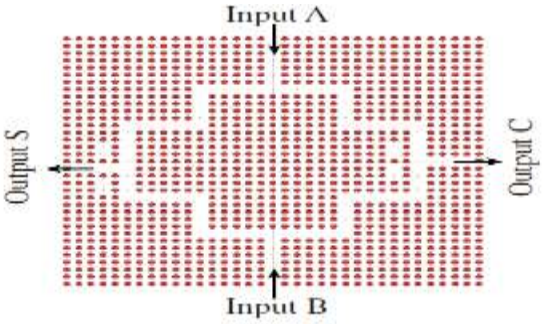

(a)

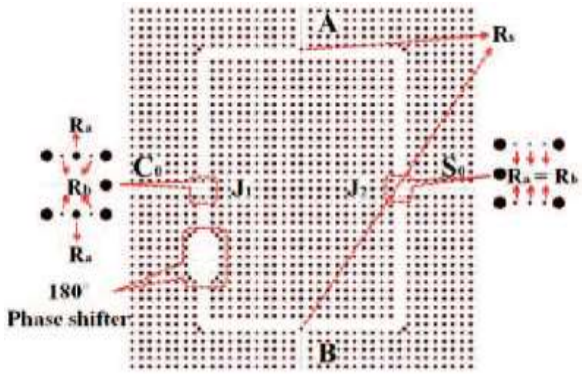

(b)

Fig. 7. The schematic diagram of the cavity of half-adder (a) [81]& (b) [89]

Table. IV was organized to display the main difference between the characteristics of (Ph. Cs.) half- adder for the proposed topologies.

TABLE.IV. COMPARISONS BETWEEN THE PUBLISHED NONLINEAR AND LINEAR ALL-OPTICAL HALF-ADDER TOPOLOGIES IN THE LITERATURE

Reference Number	Topology	Type	Simplistically	Phase Shifter	Auxiliary Inputs	Lattice Type	Size(μm2)	. Bit ate (GBPs)	Contrast Ratio (dB)	Spectral Wavelength Width (nm)
Ref [40] (2020)	ring resonators	linear	√	√	X	hexagonal	176.8	830	3.31	1250 <λ< 1910
Ref [51] (2018)		nonlinear	X	X	X	Square	1056	192.3	6.98	1304 < λ < 1890
Ref [75] (2021)		nonlinear	X	X	X	Square	379	1250	14.5	1404 <λ< 2034
Ref [86] (2013)		nonlinear	X	X	X	Square	168	746	12.78	1361.5 ≤ λ ≤ 1907.3
Ref [91] (2021)		linear	X	X	X	Square	140.1	NA	7.1	1550 < λ < 1828
Ref [50] (2018)	self-collimation	linear	X	X	X	Square	75	1100	5.4	1334.7<λ<1685.9
Ref [93] (2015)			√	√	X		277.7	NA	4.7	1332 < λ <1480
Ref [78] (2018)	Waveguides	linear	√	X	X	Square	78.38	910	16	1520<λ<1560
Ref [79] (2016)		linear	√	X	X	hexagonal	140.1	NA	5	1330 < λ < 2130
Ref [80] (2020)		linear	√	X	X	hexagonal	140.6	NA	12.55	1530 < λ < 1610
Ref [82] (2017)		nonlinear	√	X	X	Square	303	256.4	8.6	1395< λ <2657
Ref [83] (2019)		linear	√	√	X	hexagonal	137.5	4550	8.22	1380 < λ < 2240
Ref [84] (2017)		Nonlinear	X	√	X	Square	55.64	2083	3.19	1440 < λ < 2120
Ref [85] (2020)		linear	√	X	X	Square	158	2631.5	١٤	1435<λ<2105
Ref [87] (2018)		linear	X	√	√	Square	226.3	NA	16.5	1530<λ<1565
Ref [88] (2016]		linear	X	√	√	Square	102	(.2*10^-3)	NA	790 < λ < 1150
Ref [94] (2021)		linear	√	X	X	Square	158	1000	١٤	1435 <λ< 2105
Ref [81] (2019)	cavity	linear	√	√	X	Square	603.7	1270*10^3	10.95	1440 < λ < 2120
Ref [89] (2017)			√	√	X		497.8	NA	23	1441.9< λ <1631.6

From the last two sections, Table. V will summarize the figure of merits for both stated applications (i.e., decoder and half-adder). The aim is to establish bases for researchers to find the best topology that gives high quality in a particular property.

V. The General Extracted Comparative Table

As shown in table. V, it can be deduced that the ring resonator topology has the most complex structure [48, 64, 77] with the largest size [51, 71] and medium (CR) [70, 86]. It can be used in linear and nonlinear regime [72, 86]. Furthermore, it has medium bit rate.

A simple design can be obtained by using self- collimation topology with minimum size structure [50]. The linearity for its application is another figure of merit [93]. It looks like the previous topology in its medium bite rate [84]. Unfortunately, it has the worst (CR) [69].

The waveguide topology is characterized by its highest bit rate [67, 75], simple construction [78], minimum size [55], and maximum (CR) [92]. It can be found in both linear and nonlinear operations [87, 92].

From the side of view, the cavity topology has the simplest module [82]. This topology has some figure of merit such as the highest (CR) [54], high bit rate [66], and medium footprint [81]. As the material of the cavity rod can be nonlinear [83], so it can be operated in linear and nonlinear regime [83, 89].

TABLE.V. THE GENERAL EXTRACTED COMPARISON FOR THE DIFFERENT TOPOLOGIES

Face of Comparison	Ring-Resonator	Self-Collimation	Waveguide	Cavity
Type	Linear &nonlinear	Linear	Linear &nonlinear	Linear &nonlinear
Contrast ration	Medium	poor	Max normal =17	Very high
Simplest structure	Complex	Simple	Simple	Very Simple
size	Large	Min	medium	medium
Bit Rate	Medium	medium	Very high	high

VI. Conclusion

In this review, different topologies and their effect on changing the (Ph. Cs.) application were investigated. The half- adder and decoder were taken as an example to extract the various characteristics for ring resonator, self-collimation, waveguide, and cavity topologies. To operate in linear and nonlinear we can select between ring resonator, waveguide, and cavity. The higher (CR) and bit rate can be achieved from waveguide and cavity. The most topology that needs more specifications, large size, and accurate positioning is related to the ring resonator with complex construction. RSOFT, COMSOL, and other software packages are used in analysis. The dimension and location of rods are the challenges in designing (Ph. Cs.) applications for run time consumption. So, it will need some techniques to save this time and provide accurate results. The advantages and disadvantages or drawback of each topology are explained.

VII. References

[1] Yoo, H., Heo, K., Ansari, M. H. R., & Cho, S. (2021). Recent advances in electrical doping of 2d semiconductor materials: Methods,analyses and applications. In Nanomaterials (Vol. 11, Issue 4). https://doi.org/10.3390/nano11040832

[2] C. Baldauf, S. V Levchenko, P. Kratzer, and J. Neugebauer, “The Basics of Electronic Structure Theory for Periodic Systems,” Front. Chem. | www.frontiersin.org, vol. 1, 2019, doi: 10.3389/fchem.2019.00106.

[3] García de Arquer, F. P., Talapin, D. v., Klimov, V. I., Arakawa, Y., Bayer, M., & Sargent, E. H. (2021). Semiconductor quantum dots: Technological progress and future challenges. In Science (New York, N.Y.) (Vol. 373, Issue 6555). https://doi.org/10.1126/science.aaz8541

[4] E. Transport, “Density of States, Fermi Energy, and Energy Bands,” Thermoelectr. Des. Mater., pp. 189–205, 2016, doi: 10.1002/9781118848944.ch11.

[5] K. Zojer, “Simulation of Charge Carriers in Organic Electronic Devices: Methods with their Fundamentals and Applications,” Adv. Opt. Mater., vol. 9, no. 14, 2021, doi: 10.1002/adom.202100219.

[6] A. De Mauro, M. Greco, and M. Grimaldi, “A formal definition of Big Data based on its essential features,” Libr. Rev., vol. 65, no. 3, pp. 122–135, 2016, doi: 10.1108/LR-06-2015-0061.

[7] X. Zhang, Y. Wang, J. Sun, D. Liu, and D. Huang, “All-optical AND gate at 10 Gbit/s based on cascaded single-port-couple SOAs,” Opt. Express, vol. 12, no. 3, p. 361, 2004, doi: 10.1364/opex.12.000361..

[8] S. Ma, Z. Chen, H. Sun, and N. K. Dutta, “High speed all optical logic gates based on quantum dot semiconductor optical amplifiers.,” Opt. Express, vol. 18, no. 7, pp. 6417–22, 2010.

[9] J. Wang, J. Sun, and Q. Sun, “Experimental observation of a 1.5 microm band wavelength conversion and logic NOT gate at 40 Gbit/s based on sum-frequency generation.,” Opt. Lett., vol. 31, no. 11, pp. 1711–3, 2006.

[10] J. Wang, J. Sun, and Q. Sun, "Proposal for all-optical switchable OR/XOR logic gates using sum-frequency generation," IEEE Photonics Technol. Lett., vol. 19, no. 8, pp. 541–543, 2007.

[11] J. Wang et al., "PPLN-based flexible optical logic and gate," IEEE Photonics Technol. Lett., vol. 20, no. 3, pp. 211–213, 2008.

[12] M. Xiong et al., "All-optical 10 Gb/s AND logic gate in a silicon microring resonator," Opt. Express, vol. 21, no. 22, pp. 25772–25779, 2013.

[13] Rakshit, J. K., Roy, J. N., & Chattopadhyay, T. (2012). All-optical XOR/XNOR logic gate using micro-ring resonators. CODEC 2012 - 5th International Conference on Computers and Devices for Communication. https://doi.org/10.1109/CODEC.2012.6509327

[14] Vacondio, F., Sisto, M. M., Mathlouthi, W., Rusch, L. A., & LaRochelle, S. (2006). Electrical-to-optical conversion of OFDM 802.11g/a signals by direct current modulation of semiconductor optical amplifiers. 2006 International Topical Meeting on Microwave Photonics, MWP. https://doi.org/10.1109/MWP.2006.346544

[15] Joannopoulos, J. D., Johnson, S. G., Winn, J. N., & Meade, R. D. (2011). Photonic crystals: Molding the flow of light. In Photonic Crystals: Molding the Flow of Light (Second Edition).

[16] H. S. Ali and M. A. Fakhri, "An overview of Au & photonic crystal fiber of sensors," Mater. Sci. Forum, vol. 1002, 2020, doi: 10.4028/www.scientific.net/MSF.1002.282.

[17] M. De, T. K. Gangopadhyay, and V. K. Singh, "Prospects of photonic crystal fiber as physical sensor: An overview," Sensors (Switzerland), vol. 19, no. 3. 2019, doi: 10.3390/s19030464.

[18] M. R. Sardar and M. Faisal, "Methane Gas Sensor Based on Microstructured Highly Sensitive Hybrid Porous Core Photonic Crystal Fiber," J. Sens. Technol., vol. 09, no. 01, 2019, doi: 10.4236/jst.2019.91002.

[19] A. Abbaszadeh, S. Makouei, and S. Meshgini, "Highly sensitive triangular photonic crystal fiber sensor design applicable for gas detection," Adv. Electromagn., vol. 10, no. 1, 2021, doi: 10.7716/aem. v9i1.1539.

[20] F. Bozorgzadeh, D. Ahmadi, and M. Sahrai, "Innovative fiber Bragg grating filter based on a graphene photonic crystal microcavity," Appl. Opt., vol. 59, no. 1, 2020, doi: 10.1364/ao.59.000084.

[21] S. Razi and F. Ghasemi, "Broad band temperature independent photonic crystal based optical filter with response in visible wavelength range," Laser Phys., vol. 29, no. 4, 2019, doi: 10.1088/1555-6611/ab036e.

[22] A.Heydari, A. Bahrami, and A. Mahmoodi, "All-Optical XOR, XNOR, NAND and or Logic Gates Based on Photonic Crystal 3-DB Coupler for BPSK Signals," J. Opt. Commun., 2019, doi: 10.1515/joc-2018-0228.

[23] M. S. Bouaouina, M. R. Lebbal, T. Bouchemat, and M. Bouchemat, "High contrast ratio for full-designs optical logic gates based on photonic crystal ring resonator," Frequenz, vol. 74, no. 9–10, 2020, doi: 10.1515/freq-2020-0011.

[24] F. Parandin and M. M. Karkhanehchi, "Terahertz all-optical NOR and AND logic gates based on 2D photonic crystals," Superlattices Microstruct., vol. 101, 2017, doi: 10.1016/j.spmi.2016.11.038.

[25] T. S. Mostafa, N. A. Mohammed, and E. S. M. El-Rabaie, "Ultra-High bit rate all-optical AND/OR logic gates based on photonic crystal with multi-wavelength simultaneous operation," J. Mod. Opt., vol. 66, no. 9, 2019, doi: 10.1080/09500340.2019.1598587.

[26] D. Saranya and R. Anbazhagan, "Design and analysis of optical logic gates based on trifurcation structured 2D photonic crystals," Opt. Quantum Electron., vol. 52, no. 8, 2020, doi: 10.1007/s11082-020-02489-0.

[27] J. Zhang, X. -M. Xu and L. -J. He, "Three-wavelength multiplexer/demultiplexer based on photonic crystal ring resonator and cavities," 2011 Asia Communications and Photonics Conference and Exhibition (ACP), 2011, pp. 1-5, doi: 10.1117/12.903863.

[28] M. A. Ghasemi, R. Khodadadi, and H. A. Banaei, "Design And Simulation Of All Optical Multiplexer based On One-Dimensional Photonic Crystal For Optical Communications Systems," Int. J. Eng. Res. Appl., vol. 2, no. 6, pp. 960–968, 2012.

[29] S. Serajmohammadi, H. Alipour-Banaei, and F. Mehdizadeh, "Application of photonic crystal ring resonators for realizing all optical demultiplexers," Frequenz, vol. 72, no. 9–10, pp. 465–470, 2018, doi: 10.1515/freq-2017-0272.

[30] J. Smajic, C. Hafner, and D. Erni, "On the design of photonic crystal multiplexers," Opt. Express, vol. 11, no. 6, p. 566, 2003, doi: 10.1364/oe.11.000566.

[31] K. H. Hwang and G. H. Song, "Design of a high-Q channel add-drop multiplexer based on the two-dimensional photonic-crystal membrane structure," Opt. Express, vol. 13, no. 6, p. 1948, 2005, doi: 10.1364/opex.13.001948.

[32] T. S. Mostafa and E. M. El-Rabaie, "All-Optical D-Flip Flop with Multi-Wavelength Operation Based on Photonic Crystal," 2019 7th International Japan-Africa Conference on Electronics, Communications, and Computations, (JAC-ECC), 2019, pp. 184-187, doi: 10.1109/JAC-ECC48896.2019.9051118.

[33] Zamanian-Dehkordi, S. S., Soroosh, M., &Akbarizadeh, G. (2018). An ultra-fast all-optical RS flip-flop based on nonlinear photonic crystal structures. Optical Review, 25(4). https://doi.org/10.1007/s10043-018-0443-2

[34] D. G. S. Rao, "Design and implementation of All-Optical T-flip-flop using Photonic Crystals Waveguides," vol. 7, no. 4, pp. 865–870.

[35] M. Valliammai, J. Mohanraj, T. Kanimozhi, and S. Sridevi, "Design of all-optical Chalcogenide T-flip flop using Photonic Crystal Waveguide," Proc. Int. Conf. Numer. Simul. Optoelectron. Devices, NUSOD, vol. 2021-September, pp. 133–134, 2021, doi: 10.1109/NUSOD52207.2021.9541504.

[36] S. Olyaee, "Ultra-fast and compact all-optical encoder based on photonic crystal nano-resonator without using nonlinear materials," Photonics Lett. Pol., vol. 11, no. 1, 2019, doi: 10.4302/plp.v11i1.890.

[37] Z. Jiang, P. Li, and G. Xu, "Terahertz Wave 4-2 Encoder Based on Photonic Crystal," ZhongguoJiguang/Chinese J. Lasers, vol. 48, no. 20, 2021, doi: 10.3788/CJL202148.2014002.

[38] S. Naghizade and H. Khoshsima, "Low Input Power an All-Optical 4×2 Encoder based on Triangular Lattice Shape Photonic Crystal," J. Opt. Commun., vol. 42, no. 1, 2021, doi: 10.1515/joc-2018-0019.

[39] F. Mehdizadeh, M. Soroosh, and H. Alipour-Banaei, "A novel proposal for optical decoder switch based on photonic crystal ring resonators," Opt. Quantum Electron., vol. 48, no. 1, pp. 1–9, 2016, doi: 10.1007/s11082-015-0313-0.

[40] F. Parandin and M. Reza Malmir, "Reconfigurable all optical half adder and optical XOR and AND logic gates based on 2D photonic crystals," Opt. Quantum Electron., vol. 52, no. 2, 2020, doi: 10.1007/s11082-019-2167-3

[41] G. M. Paternòet al., "Integration of bio-responsive silver in 1D photonic crystals: Towards the colorimetric detection of bacteria," Faraday Discuss., vol. 223, pp. 125–135, 2020, doi: 10.1039/d0fd00026d.

[42] L. Wang et al., "All nanoparticle-based P(MMA-AA)/TiO2 one-dimensional photonic crystal films with tunable structural colors," J. Mater. Chem. C, vol. 5, no. 32, pp. 8266–8272, 2017, doi: 10.1039/c7tc02166f.

[43] H. Shen et al., "Au nanorods-sensitized 1DPC for visible detection of NIR light," J. Mater. Chem. C, vol. 5, no. 11, pp. 2942–2950, 2017, doi: 10.1039/c6tc05389k.

[44] P. Ganter and B. V. Lotsch, "Photonic nanoarchitectonics with stimuli-responsive 2D materials," Mol. Syst. Des. Eng., vol. 4, no. 3, pp. 566–579, 2019, doi: 10.1039/c8me00112j.

[45] Y. B. Yang, W. J. Wang, H. M. Fei, W. Liang, and Y. C. Wang, "Effects of structure parameters on the bandgap of two dimensional Archimedes A7 photonic crystals," Hongwai Yu HaomiboXuebao/Journal Infrared Millim. Waves, vol. 31, no. 4, pp. 306–310, 2012, doi: 10.3724/SP.J.1010.2012.00306.

[46] Liu, G. Y., Ning, Y. Q., Zhang, L. sen, Wang, W., Sun, Y. F., Qin, L., Liu, Y., & Wang, L. J. (2011). Two-dimension photonic crystal complete bandgap. FaguangXuebao/Chinese Journal of Luminescence, 32(2). https://doi.org/10.3788/fgxb20113202.0169

[47] B. Suthar, A. K. Nagar, and A. Bhargava, "Geometrical Influence on Photonic Bandgap of Three Dimensional Chalcogenide Photonic Crystals," J. Ovonic Res., vol. 6, no. 4, pp. 181–185, 2010.

[48] C. W. Chen et al., "Large three-dimensional photonic crystals based on monocrystalline liquid crystal blue phases," Nat. Commun., vol. 8, no. 1, pp. 1–8, 2017, doi: 10.1038/s41467-017-00822-y.

[49] Dhuey, S., Testini, A., Koshelev, A., Borys, N., Piper, J. R., Melli, M., Schuck, P. J., Peroz, C., & Cabrini, S. (2017). Three-dimensional woodpile photonic crystals for visible light applications. Journal of Physics Communications, 1(1). https://doi.org/10.1088/2399-6528/aa7ef9

[50] M. R. Jalali-Azizpoor, M. Soroosh, and Y. Seifi-Kavian, "Application of self-collimated beams in realizing all-optical photonic crystal-based half-adder," Photonic Netw. Commun., vol. 36, no. 3, pp. 344–349, 2018, doi: 10.1007/s11107-018-0786-4.

[51] S. Serajmohammadi, H. Alipour-Banaei, and F. Mehdizadeh, "Proposal for realizing an all-optical half adder based on photonic crystals," Appl. Opt., vol. 57, no. 7, p. 1617, 2018, doi: 10.1364/ao.57.001617.

[52] M. Moradi, M. Mohammadi, S. Olyaee, and M. Seifouri, "Design and Simulation of a Fast All-Optical Modulator Based on Photonic Crystal Using Ring Resonators," pp. 765–771, 2022.

[53] Y. Zheng, Q. Wang, M. Lin, and Z. Ouyang, "Enhancement of Self-Collimation Effect in

Photonic Crystal Membranes Using Hyperbolic Metamaterials," 2022.

[54] M. J. Maleki and M. Soroosh, "A novel proposal for performance improvement in two-dimensional photonic crystal-based 2-To-4 decoders," Laser Phys., vol. 30, no. 7, 2020, doi: 10.1088/1555-6611/ab9089.

[55] A. Heydari and A. Bahrami, "All-optical half adder based on photonic crystals for BPSK signals," Opt. Quantum Electron., vol. 50, no. 5, pp. 1–9, 2018, doi: 10.1007/s11082-018-1477-1.

[56] Anagha, E. G., & Jeyachitra, R. K. (2022). Optimized design of an all-optical XOR gate with high contrast ratio and ultra-compact dimensions. Applied Physics B: Lasers and Optics, 128(2). https://doi.org/10.1007/s00340-021-07747-x

[57] "Photonic Design Software | RSoft Products", Synopsys.com, 2019. [Online]. Available: https://www.synopsys.com/optical-solutions/rsoft.html. [Accessed: 05- Jan- 2022].

[58] "COMSOL Multiphysics® Software - Understand, Predict, and Optimize", COMSOL Multiphysics©, 2019. [Online]. Available: https://www.comsol.com/comsol-multiphysics. [Accessed: 05- Jan- 2022].

[59] T. S. Mostafa, "All-Optical D-Flip Flop with Multi-Wavelength Operation Based on Photonic Crystal," pp. 192–195, 2019.

[60] M. M. Mano, "Digital Logic And Computer Design By M. Morris Mano (PDF Drive)." 2017.

[61] G. Keiser, *Optical Fiber Communications*, 4th ed. McGraw-Hill Education, 2010.

[62] F. Mehdizadeh and H. Alipour-banaei, "All optical 1 to 2 decoder based on photonic crystal ring resonator," J. Optoelectron. Nanostructures, vol. 2, no. 1, pp. 1–10, 2017.

[63] S. Serajmohammadi, H. Alipour-Banaei, and F. Mehdizadeh, "All optical decoder switch based on photonic crystal ring resonators," Opt. Quantum Electron., vol. 47, no. 5, pp. 1109–1115, 2015, doi: 10.1007/s11082-014-9967-2.

[64] S. Khosravi and M. Zavvari, "Design and analysis of integrated all-optical 2 × 4 decoder based on 2D photonic crystals," Photonic Netw. Commun., vol. 35, no. 1, pp. 122–128, 2018, doi: 10.1007/s11107-017-0724-x.

[65] A. Rostamizadeh, M. Taghizadeh, J. Jamali, and A. Andalib, "Application of photonic crystal based nonlinear ring resonators for realizing all optical 3-to-8 decoder," J. Opt. Commun., pp. 2–9, 2020, doi: 10.1515/joc-2020-0094.

[66] T. A. Moniem, "All optical active high decoder using integrated 2D square lattice photonic crystals," J. Mod. Opt., vol. 62, no. 19, pp. 1643–1649, 2015, doi: 10.1080/09500340.2015.1061061.

[67] H. Mondal, M. Sen, and K. Goswami, "Design and analysis of all-optical 1-to-2 line decoder based on linear photonic crystal," IET Optoelectron., vol. 13, no. 4, pp. 191–195, 2019, doi: 10.1049/iet-opt.2018.5099.

[68] T. Daghooghi, M. Soroosh, and K. Ansari-Asl, "A novel proposal for all-optical decoder based on photonic crystals," Photonic Netw. Commun., vol. 35, no. 3, pp. 335–341, 2018, doi: 10.1007/s11107-017-0746-4

[69] H. Alipour-Banaei, M. GhorbanzadehRabati, P. Abdollahzadeh-Badelbou, and F. Mehdizadeh, "Effect of self-collimated beams on the operation of photonic crystal decoders," J. Electromagn. Waves Appl., vol. 30, no. 11, 2016, doi: 10.1080/09205071.2016.1202785.

[70] T. Daghooghi, M. Soroosh, and K. Ansari-Asl, "Ultra-fast all-optical decoder based on nonlinear photonic crystal ring resonators," Appl. Opt., vol. 57, no. 9, p. 2250, 2018, doi: 10.1364/ao.57.002250.

[71] H. Alipour-Banaei, F. Mehdizadeh, S. Serajmohammadi, and M. Hassangholizadeh-Kashtiban, "A 2∗4 all optical decoder switch based on photonic crystal ring resonators," J. Mod. Opt., vol. 62, no. 6, pp. 430–434, 2015, doi: 10.1080/09500340.2014.957743.

[72] A. Rostamizadeh, M. Taghizadeh, J. Jamali, and A. Andalib, "Ultra-fast all optical decoder using photonic crystal based nonlinear ring resonators," Opt. Quantum Electron., vol. 52, no. 2, 2020, doi: 10.1007/s11082-020-2221-1.

[73] T. Daghooghi, M. Soroosh, and K. Ansari-Asl, "A low-power all optical decoder based on photonic crystal nonlinear ring resonators," Optik (Stuttg)., vol. 174, pp. 400–408, 2018, doi: 10.1016/j.ijleo.2018.08.090.

[74] F. Mehdizadeh, H. Alipour-Banaei, and S. Serajmohammadi, "Design and simulation of all optical decoder based on nonlinear PhCRRs," Optik (Stuttg)., vol. 156, pp. 701–706, 2018, doi: 10.1016/j.ijleo.2017.12.011.

[75] D. Based, C. Structures, M. J. Maleki, and M. Soroosh, "Improving the Performance of 2-To-4 Optical," pp. 1–9, 2019

[76] H. M. E. Hussein, T. A. Ali, and N. H. Rafat, "A review on the techniques for building all-optical photonic crystal logic gates," *Opt. Laser Technol.*,

vol. 106, pp. 385–397, 2018, doi: 10.1016/j.optlastec.2018.04.018.

[77] P. K. RAMA, K. R. ARUN, and S. ROBINSON, "Design and Analysis of All Optical Half Adder Based on Two Dimensional Photonic Crystals," i-manager's J. Digit. Signal Process., vol. 6, no. 4, p. 27, 2018, doi: 10.26634/jdp.6.4.16266.

[78] Q. Liu and Z. B. Ouyang, "All-optical half adder based on cross structures in two-dimensional photonic crystals," GuangziXuebao/Acta Photonica Sin., vol. 37, no. SUPPL. 2, pp. 46–50, 2008, doi: 10.1364/oe.16.018992.

[79] M. M. Karkhanehchi, F. Parandin, and A. Zahedi, "Design of an all optical half-adder based on 2D photonic crystals," Photonic Netw. Commun., vol. 33, no. 2, pp. 159–165, 2017, doi: 10.1007/s11107-016-0629-0.

[80] R. Sivaranjaniet al., "Photonic crystal based all-optical half adder: A brief analysis," Laser Phys., vol. 30, no. 11, 2020, doi: 10.1088/1555-6611/abbe8b.

[81] C. Lu et al., "All-optical logic gates and a half-adder based on lithium niobate photonic crystal micro-cavities," Chinese Opt. Lett., vol. 17, no. 7, p. 072301, 2019, doi: 10.3788/COL201917.072301.

[82] M. Neisy, M. Soroosh, and K. Ansari-Asl, "All optical half adder based on photonic crystal resonant cavities," Photonic Netw. Commun., vol. 35, no. 2, pp. 245–250, 2018, doi: 10.1007/s11107-017-0736-6.

[83] M. Seifouri, S. Olyaee, M. Sardari, and A. Mohebzadeh-Bahabady, "Ultra-fast and compact all-optical half adder using 2D photonic crystals," IET Optoelectron., vol. 13, no. 3, pp. 139–143, 2019, doi: 10.1049/iet-opt.2018.5130.

[84] S. C. Xavier, K. Arunachalam, E. Caroline, and W. Johnson, "Design of two-dimensional photonic crystal-based all-optical binary adder," Opt. Eng., vol. 52, no. 2, p. 025201, 2013, doi: 10.1117/1.oe.52.2.025201.

[85] S. Naghizade and H. Saghaei, "A Novel Design for an All-Optical Half Adder Using Linear Defects in Photonic Crystal Microstructure," J. Appl. Res. Electr. Eng., vol. 1, no. 1, pp. 8–13, 2021, doi: 10.22055/jaree.2020.34466.1010.

[86] M. Ghadrdan and M. A. Mansouri-Birjandi, "Concurrent implementation of all-optical half-adder and AND& XOR logic gates based on nonlinear photonic crystal," Opt. Quantum Electron., vol. 45, no. 10, pp. 1027–1036, 2013, doi: 10.1007/s11082-013-9713-1.

[87] E. H. Shaik and N. Rangaswamy, "Design of all-optical photonic crystal half adder with T-shaped waveguides using path difference based interference," Prog. Electromagn. Res. Symp., vol. 2017-November, pp. 2596–2602, 2017, doi: 10.1109/PIERS-FALL.2017.8293574.

[88] S. Swarnakar, S. Kumar, and S. Sharma, "All-Optical Half-Adder Circuit Based on Beam Interference Principle of Photonic Crystal," J. Opt. Commun., vol. 39, no. 1, pp. 13–17, 2017, doi: 10.1515/joc-2016-0121

[89] E. H. Shaik and N. Rangaswamy, "Implementation of photonic crystal based all-optical half adder using T-shaped waveguides," Proc. 2017 2nd Int. Conf. Comput. Commun. Technol. ICCCT 2017, pp. 148–150, 2017, doi: 10.1109/ICCCT2.2017.7972259.

[90] Naghizade, saleh, & Saghaei, H. (2021). Ultra-fast tunable optoelectronic half adder/subtractor based on photonic crystal ring resonators covered by graphene nanoshells. Optical and Quantum Electronics, 53(7). https://doi.org/10.1007/s11082-021-03071-y

[91] M. Moradipour, P. KazemiEsfeh, and Z. Alaie, "Investigating the plasmonic effect on half adder and full adder based on photonic crystal," Opt. Quantum Electron., vol. 53, no. 1, pp. 1–17, 2021, doi: 10.1007/s11082-020-02645-6.

[92] C. Engineering, "Design and Implementation of Optical Half-Adder for Switching Purpose," vol. 12, no. 07, pp. 371–380, 2021

[93] Y. C. Jiang, S. Bin Liu, H. F. Zhang, and X. K. Kong, "Realization of all optical half-adder based on self-collimated beams by two-dimensional photonic crystals," Opt. Commun., vol. 348, pp. 90–94, 2015, doi: 10.1016/j.optcom.2015.03.011.

[94] S. Naghizade and H. Saghaei, "A novel design of all-optical half adder using a linear defect in a square lattice rod-based photonic crystal microstructure," 2020